

N O T I C E

THIS DOCUMENT HAS BEEN REPRODUCED FROM
MICROFICHE. ALTHOUGH IT IS RECOGNIZED THAT
CERTAIN PORTIONS ARE ILLEGIBLE, IT IS BEING RELEASED
IN THE INTEREST OF MAKING AVAILABLE AS MUCH
INFORMATION AS POSSIBLE

HEAT BALANCE OF THE EARTH

M. I. Budyko, T. G. Berlyand, N. A. Yefimova, L. I.
Zuberok, L. A. Strokina

Translation of "Teplovoy balans zemli"
Leningrad, Gidrometeoizdat, 1978,
pp 1-41

(NASA-TM-75826) HEAT BALANCE OF THE EARTH
(National Aeronautics and Space
Administration) 55 p HC A04/MF A01 CSCL 08E

N81-13387

Unclas
G5/42 29453

NOTICE: BECAUSE OF COPYRIGHT RESTRICTION THIS
TRANSLATION HAS NOT BEEN PUBLISHED. THIS COPY IS
FOR INTERNAL USE OF NASA PERSONNEL AND ANY REFERENCE
TO THIS PAPER MUST BE TO THE ORIGINAL FOREIGN SOURCE.



NATIONAL AERONAUTICS AND SPACE ADMINISTRATION
WASHINGTON, D.C. 20546 APRIL 1980

STANDARD TITLE PAGE

1. Report No. NASA TM-75826	2. Government Accession No.	3. Recipient's Catalog No.	
4. Title and Subtitle HEAT BALANCE OF THE EARTH		5. Report Date APRIL 1980	6. Performing Organization Code
		7. Author(s) M. I. Budyko, T. G. Berlyand, N. A. Yefimova, L. I. Zubenok, L. A. Strokina	8. Performing Organization Report No.
9. Performing Organization Name and Address SCITRAN Box 5456 Santa Barbara, CA 93108		10. Work Unit No.	
		11. Contract or Grant No. NASW-3198	12. Type of Report and Period Covered Translation
12. Sponsoring Agency Name and Address National Aeronautics and Space Administration Washington, D.C. 2054		13. Sponsoring Agency Code	
14. Supplementary Notes Translation of "Teplovo balans zemli," Leningrad Gidrometeoizdat, 1978, pp 1-41, (A78-46579)			
15. Abstract Results of improved calculations of the heat balance components of earth's surface are reported for yearly average conditions. The technique used to determine the heat-balance components from land-and sea-based actinometric observations as well as from satellite data on the radiation balance of the earth-atmosphere system is described in detail, with special attention given to short-wavelength solar radiation on the continents, effective radiation from the land surface, the radiation balance of the ocean surface, heat expended by both evaporation from the ocean surface and turbulent heat transfer between the ocean surface and the atmosphere. World maps of heat-balance components are presented which show yearly average values of total radiation, radiation balance, heat expended by evaporation, the turbulent heat flow between earth's surface and atmosphere, and heat transfer between the ocean surface and underlying waters. The global surface heat balance is estimated along with global values of the various components and the heat-balance components for different latitude zones.			
17. Key Words (Selected by Author(s))		18. Distribution Statement Limited to United States Government Agencies and Contractors	
19. Security Classif. (of this report) Unclassified	20. Security Classif. (of this page) Unclassified	21. No. of Pages 54	22.

TABLE OF CONTENTS

	Page
1. Introduction	1
2. Method of Determining Components of Heat Balance	3
2.1. Short wave radiation on the continents	3
2.2. Effective radiation of the surface of the land.	7
2.3. Radiation balance of the surface of the oceans	10
2.4. Loss of heat in evaporation from the surface of the land.	13
2.5. Heat loss to evaporation from the ocean surface and turbulent heat exchange between the ocean surface and the atmosphere	20
3. World Maps for the Heat Balance Components	23
3.1. Total radiation	23
3.2. Radiation balance	27
3.3. Heat Loss to Evaporation	31
3.4. Turbulent Heat Flux Between the Earth's Surface and the Atmosphere	37
3.5. Heat Exchange Between the Surface of the Ocean and the Underlying Water Layers	41
4. Heat Balance of the Earth	45
5. References	48

1. Introduction

43*

Research on the heat balance of the earth began in the nineteenth century, when actinometric devices were developed and calculations were made of changes in solar radiation, reaching the outer boundary of the earth, as a function of the latitude and time of year. In the first half of the twentieth century V. Schmidt, A. Ongster, F. Albröcht, and S. I. Savinov determined the components of the heat balance of the earth's surface for separate regions of the earth.

In 1945-1974 in the Main Geophysical Observatory. im. A. I. Voyeykov, research was carried out on the heat balance of the earth. This led to the formulation of world maps of the components of the heat balance of the earth's surface for each month and for the average yearly conditions, which were published in the "Atlas of the Heat Balance" [5]. As a result of later research, these maps were greatly refined and augmented together with several maps of components of the heat balance of the Earth-atmosphere system, which were published in "Atlas of the Heat Balance of the Earth" [6].

During the period after the publication of the second atlas of heat balance, a great deal of material was accumulated from actinometric observations on the continents, performed in regions where previously there were no actinometric stations. During these years, of great importance was the extensive material from actinometric observations on the ocean, which made it possible to establish the features of the radiation mode of bodies of water.

A great deal of attention should be given to the results of satellite observations recently performed on the characteristics of the radiation mode, which have been repeatedly used to draw up world maps of the absorbed radiation and the radiation balance of

* Numbers in margins indicate foreign pagination.

the Earth-atmosphere system.

The development of studies on turbulent diffusion made it possible to refine the methods previously used to calculate the heat lost in evaporation and turbulent heat exchange of the Earth's surface with the atmosphere for the oceans.

The accumulation of observational material and the development of computational methods to determine the components of the heat balance made it possible to draw up new world maps ⁴ in 1975 of the components of the heat balance, which were more accurate as compared with maps published previously.

This problem was particularly pressing due to the fact that in the last 10-15 years there has been wide use of materials on the heat balance in studies of the theory of the climate, in studies of the water balance, and in studies of many other problems of meteorology, hydrology of land and oceanology.

This study publishes several world maps of the components of the heat balance of the Earth's surface for average yearly conditions.¹ The materials shown on these maps have been used in investigating the world's water balance [31] and in studies on the theory of the heat mode of the atmosphere.

The new information on the heat balance of the Earth's surface, along with materials from satellite observations on the radiation balance of the Earth-atmosphere system made it possible to refine the picture of the heat balance of the Earth, which is given in a final form in this study.

¹ I.M. Beyev, O.D. Okhotin, Ye. F. Seleznev, Ye. Ye. Sibir, N. I. Smirnov, Ye. M. Polynskaya participated in the difficult calculations of the components of heat balance.

2. Method of Determining Components of Heat Balance

2.1. Short wave radiation on the continents

The arrival of the total solar radiation on the surface of the Earth depends upon the latitude of the location, the declination of the Sun, the state of the atmosphere (transparency, cloudiness) and the nature of the underlying surface (albedo).

At the present time there is a great amount of observational data on the total radiation although there are regions where the number of actinometric stations is small. This is due to the fact that to obtain the necessary information it is required to use indirect methods of calculating the total radiation. These methods are based on semi-empirical relationships making it possible to calculate the solar radiation based on materials from network measurements of the basic meteorological elements [10, 35].

The formulas for determining the total radiation Q , obtained on the basis of processing observational data, usually express its dependence on the solar radiation which either reaches the upper boundary of the Earth (Q_A) or the surface of the Earth under the condition of a cloudless sky (Q_0), and /5 also on the amount of cloudiness or the duration of the sunshine S .

The study [9] reached the conclusion that the relationship between the total radiation and the amount of clouds may be described with sufficient accuracy by a relationship of the type

$$\frac{Q}{Q_0} = 1 - (a + bn)n, \quad (1)$$

where a and b are empirical coefficients. Thus the average values of the coefficient a were found for different latitudes and it was shown that the coefficient b may be assumed to be constant.

This formula was used when calculating the initial data lying at the basis of the world monthly maps of the total solar radiation given in previous studies [1, 3].

During the years after the publication of the "Atlas of the Heat Balance of the Earth" [6], there was a great increase in the material from actual observations on the total radiation, especially for the tropical and polar latitudes. This made it possible to verify and refine the parameters in formula (1).

To use this relationship, it is necessary to obtain very reliable values for the total solar radiation under the condition of a cloudless sky. This value was found previously [3] using a method proposed by V. N. Ukraintsev. To obtain the latitudinal behavior of the average monthly values of Q_0 , material from 70 stations was used. These stations were located on land primarily at latitudes outside the tropical latitudes of the Earth.

To refine the dependence obtained previously for the possible solar radiation in the case of a cloudless sky on the latitude, this study used the daily data from 190 points distributed uniformly over the continents, which greatly increased the volume of material previously used.

Table 1 gives the refined average monthly values of the possible total radiation for different latitudes of the northern and southern hemispheres.

An estimate of the deviations of the values Q_0 , pertaining to individual points, from the average latitudinal values showed that these fluctuated from 3-7%. When comparing the results given in this table with the data obtained previously [9], it was found that in the middle and lower latitudes the new values were less than the previous values by 4-5% on the average. In the polar latitudes they increased: in the northern hemisphere, this increase was 2-4%, in the southern hemisphere, in certain autumn months, it reached 10-12%. The great refinement in the value of Q_0 for the high latitudes of the southern hemisphere was due to the development in the last 15 years of an actinometric network in the Antarctic.

16

TABLE 1. LATITUDINAL DISTRIBUTION OF THE TOTAL RADIATION UNDER CONDITIONS OF A CLOUDLESS SKY
 Q_0 (kcal./cm² * month)*

Latitude	I	II	III	IV	V	VI	VII	VIII	IX	X	XI	XII
90° N	0	0	0.3	10.0	20.8	25.8	21.2	14.0	2.4	0	0	0
80	0	0	2.4	10.1	20.4	24.9	22.6	11.2	4.6	0.5	0	0
70	0.03	1.4	5.7	12.6	19.5	22.8	21.2	14.7	7.5	2.7	0.3	0
60	1.8	4.5	9.4	11.9	19.8	22.2	21.0	16.2	10.9	6.1	2.4	1.1
50	4.8	7.6	12.8	17.3	20.9	22.6	21.8	18.2	14.0	9.7	5.5	4.0
40	8.2	11.2	15.6	19.4	22.0	23.1	22.4	20.1	16.4	12.8	8.8	7.3
30	11.5	14.6	17.6	20.5	22.2	22.8	22.4	20.9	18.3	15.2	12.2	10.6
20	14.6	16.6	19.1	20.8	21.6	21.8	21.7	20.9	19.4	17.4	15.2	13.9
10	17.2	18.6	20.2	20.7	20.2	19.9	20.1	20.5	20.2	19.1	17.6	16.7
0	19.4	20.1	20.7	20.0	18.7	18.0	18.2	19.5	20.2	20.4	19.7	19.1
10° S	21.2	20.9	20.6	18.7	16.6	15.6	16.0	17.7	19.7	20.9	21.3	21.2
20	22.4	21.3	19.8	16.7	14.2	12.8	13.5	15.6	18.7	20.6	22.2	22.6
30	23.1	21.0	18.2	14.2	11.2	9.8	10.3	13.1	17.0	19.9	22.5	23.8
40	23.5	20.2	16.0	11.7	8.3	6.6	7.4	10.1	14.5	18.4	22.3	24.6
50	23.3	18.9	13.7	8.8	5.3	3.6	4.2	6.8	11.7	16.6	21.8	24.7
60	23.1	17.0	10.7	5.6	2.4	1.0	1.6	3.8	8.5	14.1	20.9	24.3
70	23.4	15.1	7.3	2.2	0.2	0	0	1.0	4.9	11.6	21.3	25.7
80	24.4	14.3	4.8	0.1	0	0	0	0	2.0	9.7	21.9	27.4
90	25.2	14.1	3.0	0	0	0	0	0	0.3	8.8	22.2	28.0

* Translator's Note: Commas represent decimal points

As has already been noted, when calculating the total radiation some researchers did not use the value of Q_0 , but data on the solar radiation reaching the upper boundary of the atmosphere Q_A . The average latitudinal values of these quantities are given in Table 2 for the northern hemisphere.

TABLE 2. LATITUDINAL DISTRIBUTION OF THE SOLAR RADIATION REACHING THE UPPER BOUNDARY OF THE ATMOSPHERE Q_A kcal/(cm² · month).

Latitude	I	II	III	IV	V	VI	VII	VIII	IX	X	XI	XII
90° N	0	0	1.0	13.8	26.3	31.7	29.0	19.2	4.6	0	0	0
80	0	0	3.2	14.3	25.9	31.3	28.8	19.2	6.8	0.7	0	0
70	0.1	2.2	7.9	16.8	25.1	29.7	27.4	20.0	11.3	4.1	0.4	0
60	2.6	6.1	12.3	19.5	25.9	29.0	27.4	22.0	15.2	8.4	3.6	1.7
50	6.6	10.4	16.2	22.3	27.2	29.4	28.4	24.5	18.7	12.6	7.8	5.6
40	11.0	14.6	19.6	21.6	28.1	29.6	28.8	26.1	21.7	16.6	11.8	9.9
30	15.3	18.4	22.5	26.1	28.3	29.2	28.8	27.1	24.0	20.3	16.2	14.2
20	19.2	21.8	24.6	26.8	27.8	28.1	28.0	27.4	25.6	23.0	20.1	18.4
10	22.8	24.5	26.1	26.8	27.0	26.8	26.8	26.8	26.5	25.2	23.4	22.2
0	25.7	26.5	26.7	25.9	24.6	23.7	21.2	25.4	26.5	26.7	28.0	25.3

The estimate of the relationships between Q_0 and Q_A show that the attenuation of the solar radiation in a cloudless atmosphere due to its absorption and scattering is about 25% for the year.

/7

Using the new material on the values of the coefficient b given in formula (1), verification confirmed the values assumed earlier.

As already noted, allowance for the influence of cloudiness on solar radiation reaching the surface of the Earth may be made by a two-sided method: directly from visual data on the amount of clouds or with the use of instrument observations -- recording the duration of the solar illumination.

In the equatorial and tropical regions, where the actinometric network is widely spaced, apart from data on cloudiness, a large volume of material on heliographic observations has been accumulated, making it possible to use the dependence between the total radiation and the relative duration of solar illumination for conditions at low latitudes. For this purpose

the corresponding data on Africa, Asia, and Australia were given. The results of the calculations confirmed the occurrence of a linear relationship, obtained previously by Ongster using observational materials in the moderate zone [44] in the form

$$\frac{Q}{Q_0} = 0.25 + 0.75 \frac{S}{S_0}. \quad (2)$$

A comparison of the average monthly values of the total radiation, calculated based on data from the heliographic network of South America, with the data of actual observations showed that the computational errors did not exceed 8-10%.

In this study when it was necessary to include materials from an indirect calculation of the total radiation, primarily the relationship (2) was used, since data on the duration of the solar illumination are more reliable than visual observations on the cloudiness.

To determine the absorbed solar radiation, it is necessary to use data on the reflective capacity (Albedo) of different natural surfaces of the Earth. A comparison of the values of albedo, used when formulating the maps of the "Atlas of the Heat Balance of the Earth" [6], with data obtained by several authors in the last fifteen years confirmed the great accuracy of the values given in the atlas, with the exception of the values for the tropical forest, whose albedo, based on new measurements [49] is 12%. This was used in this study when calculating the absorbed radiation.

2.2. Effective radiation of the surface of the land.

To determine the radiation of the Earth's surface R , which represents the difference between the absorbed shortwave solar/8

radiation and the effective radiation

$$R = Q(1 - \alpha) - I, \quad (3)$$

in addition to materials on the total solar radiation Q and the total albedo α , data are necessary on the effective radiation I , which represents the difference between the long wave radiation of the underlying surface and the absorbed portion of the oncoming radiation of the atmosphere. Because of the fact that there are no mass data on the fluxes of long wave radiation at stations of the worldwide actinometric network, for determining the effective radiation, theoretical and semi-empirical methods are used which consider the dependence of the effective radiation on the temperature of the emitting surface, the temperature, and the humidity of the air and cloudiness. When determining the values of the radiation balance, which lie at the basis of previously published maps [5, 6], to calculate the effective radiation, a method was used developed in the Main Geophysical Observatory [8] and was refined based on observational materials from the actinometric stations of the USSR [21].

Based on the existing observational materials (basically the actinometric stations of the Soviet Union) the values of the effective radiation are determined as the difference of the shortwave and total radiation balances, and consequently include measurement errors for these elements. In addition to random errors, there is a systematic value of the effective radiation which is too low due to the lower sensitivity of the thermoelectric balance meters to long wave radiation, as compared with shortwave, which is used to calibrate the equipment. Based on an estimate of Yu. D. Yanishevskiy, the value of the systematic error of the thermoelectric balance meters when measuring the long wave radiation is about 8-10%. When refining the dependence of the effective radiation on the elasticity of water vapor based

on observational materials from actinometric stations of the USSR, this systematic error was taken into account by increasing the effective radiation by 8% in the case of a cloudless sky [21].

The formula found previously [6,22] for calculating the average sums over many months of the effective radiation has the form

$$I = s\sigma^4(11.4 - 0.23\epsilon)(1 - cn) + \Delta I, \quad (4)$$

where θ , e , n are the average monthly values of the temperature of the air (K), the elasticity of water vapor (mb), and the total cloudiness (portions of a unit); c - coefficient considering the influence of cloudiness for radiation [6,22]; s - integral radiation capacity of the surface of land, equaling 0.95; σ - Stephan-Boltzmann constant ($\text{cal}/\text{cm}^2 \cdot \text{min} \cdot \text{K}^4$); ΔI - correction for effective radiation proportional to the temperature difference between the underlying surface (Q_s) and the air (θ). ΔI determined according to the heat balance method [22]:

$$\Delta I = 4s\sigma^3(\theta_s - \theta) = \frac{R_0 - LE - B}{1 + \frac{pc_p D}{4s\sigma^3}}. \quad (5)$$

The forms used for the dependence of effective radiation on cloudiness and the temperature difference between the underlying surface and the air were confirmed by materials from actinometric observations of the network of USSR stations. A determination was also made of the error of calculating the monthly values of the effective radiation using the values of meteorological elements in formula (4) for different averaging periods. As was shown in [23] the error due to using the average monthly values of the meteorological elements was less than 1% in almost 90% of the cases, i.e., one order of magnitude less than the errors for the method of determining the monthly sums of effective radiation.

A comparison made for 50 stations in the Soviet Union¹ showed that the differences in the calculated and measured [37] yearly sums of effective radiation did not exceed 10% in 60% of the cases and were less than 15% in 80% of the cases. The differences in the yearly sums of the radiation balance, obtained by calculations and from observational data, did not exceed 10% in 55% of the cases and 15% in 75% of the cases.

It follows from the existing materials that the average error of the calculated sums of the radiation balance is about 10%.

2.3. Radiation balance of the surface of the oceans

The radiation balance of the surface of the world's ocean was determined by calculations using a method developed on the basis of generalizing materials from ship actinometric observations [20]. The following formula was used for this calculation

$$R = Q_0 f(n) - [s \frac{t_w}{\sigma} - s l_{\infty} (1 + kn^m)] \quad (6)$$

where Q_0 is the total solar radiation for a cloudless sky (pos-

¹These stations were located in different climatic zones on the European part of the USSR (Arkhangel'sk, Kargopol', Voyeykovo Tartu, Gork'iy, Moscow, Minsk, Pinsk, Vasilevichi, Kursk, Kamen-naya Step', Kuybyshev, Kiev, Poltava, Voigograd, Kishinev, Odessa, Sal'sk, Astrakhan', Sochi) and on the Asian part of the USSR (Olenok, Salekhard, Srednekolymsk, Turukhansk, Oymyakon, Markovo, Verkhoyansk, Yeniseysk, Yakutsk, Aldan, Vysokaya Dub-rava, Omsk, Novosibirsk, Kirensk, Irkutsk, Skovorodino, Borzya, Chita, im. Poliny Osepenko, tundra, Tselinograd, Semipalatinsk, Khabarovsk, F. Shevchenko, Aral'skoye More, Alma-Ata, Tashkent, Sad-Gorod, Dushanbe, Ashkhabad, Termez).

sible radiation); $f(n)$ - function, determined by the dependence of the total radiation on the cloudiness; α - albedo of the surface of the ocean; s - integral radiation capacity of a water surface which equals 0.91; t_w - temperature of the water surface in degrees Kelvin; I_{at} - radiation of the atmosphere for a cloudless sky; n - total cloudiness in points; k, m - parameters considering the influence of cloudiness upon the radiation of the atmosphere; β - empirical coefficient considering the difference between $\frac{1}{n}$ and $\frac{1}{n^2}$.

The values of the total solar radiation for a cloudless sky Q_0 were calculated as a function of the solar altitude at fixed intervals of the atmospheric transparency coefficient p_2 . The study [20] gave the values of the possible total radiation at $p_2 = 0.75$. The following relation was used to change to the daily sums for other values of the atmospheric transparency coefficient

$$Q_0 = a Q_{0,75} \quad (7)$$

where the coefficient a characterizes the influence of different midday heights of the sun and the transparency coefficients p_2 .

The use of the atmospheric transparency conditions over the world's ocean showed differences in the values of p_2 in individual oceans. It was found that the values of p_2 in the Pacific and Indian Oceans were similar, whereas in the Atlantic they were less, particularly at the equatorial and tropical latitude, due to a differing influence upon the atmosphere of the surrounding oceans of the continents [19]. Taking these differences into account, tables were drawn up for the average latitudinal values of the monthly sums of possible radiation, characterized for the Atlantic Ocean [Table 3], Pacific Ocean and the Indian Oceans [Table 4].

TABLE 3. MONTHLY SUMS OF POSSIBLE TOTAL RADIATION FOR THE ATLANTIC OCEAN (kcal/(cm² · month))

Latitude	I	II	III	IV	V	VI	VII	VIII	IX	X	XI	XII
60° N	1,6	4,0	9,1	14,7	20,4	21,9	21,3	16,9	10,9	6,0	2,3	1,0
50	4,4	6,9	12,2	16,7	21,0	21,8	21,5	18,2	13,2	9,0	5,2	3,3
40	7,5	9,6	14,6	18,0	21,4	21,7	21,6	19,3	15,3	11,8	8,1	6,8
30	10,5	12,1	16,6	19,0	21,3	21,0	21,3	19,9	16,8	14,4	11,0	9,7
20	13,6	14,3	18,1	19,3	20,7	20,0	20,5	19,9	18,0	16,4	13,6	12,5
10	16,2	16,2	19,3	19,2	19,6	18,7	19,2	19,5	18,7	18,2	15,7	15,5
0	18,7	17,6	19,7	18,6	17,9	16,7	17,5	18,5	18,8	19,5	18,2	18,3
10° S	20,6	18,4	19,7	17,5	16,0	14,4	15,4	17,3	18,5	20,3	20,3	20,6
20	22,0	19,2	19,2	15,8	13,6	11,7	12,8	15,3	17,3	20,5	21,1	22,2
30	22,9	19,2	18,0	13,8	10,9	8,7	9,9	12,9	15,8	19,9	21,6	23,3
40	23,4	18,7	16,3	11,4	8,0	6,2	7,1	10,9	13,9	19,0	21,8	24,2
50	23,8	18,0	14,5	8,8	5,2	3,4	4,2	7,4	11,7	17,8	21,7	24,9
60	23,8	16,8	11,9	6,2	2,4	1,0	1,6	4,4	9,2	16,2	20,9	25,2

TABLE 4. MONTHLY SUMS OF THE POSSIBLE TOTAL RADIATION FOR THE PACIFIC AND INDIAN OCEANS (kcal/(cm² · month)).

Latitude	I	II	III	IV	V	VI	VII	VIII	IX	X	XI	XII
60° N	1,7	4,1	9,3	14,9	20,6	22,1	21,3	17,1	11,1	6,1	2,4	1,2
50	4,4	6,9	12,4	17,0	21,4	22,3	22,1	18,7	13,6	9,3	5,3	3,5
40	7,7	9,8	14,9	18,5	22,0	22,3	22,3	19,9	15,7	12,4	8,4	6,9
30	10,9	12,4	17,1	19,5	21,9	21,6	22,0	20,5	17,3	14,9	11,5	10,1
20	14,0	14,7	18,7	19,9	21,3	20,7	21,3	20,6	18,6	17,0	14,2	13,3
10	16,8	16,8	19,9	19,7	20,2	19,2	19,9	20,2	19,3	18,8	16,6	16,3
0	19,4	18,2	20,4	19,1	18,5	17,2	18,0	19,1	19,3	20,0	18,8	18,9
10° S	21,2	19,1	20,4	18,0	16,5	14,9	15,8	17,6	18,9	20,8	20,4	21,1
20	22,4	19,7	19,7	16,3	14,0	12,1	13,1	15,7	17,7	20,8	21,5	22,8
30	23,4	19,6	18,4	14,2	11,2	9,1	10,2	13,2	16,1	20,4	21,9	23,8
40	23,8	18,9	16,6	11,7	8,2	6,3	7,2	10,3	14,0	19,2	22,0	24,5
50	23,8	18,0	14,5	8,7	5,2	3,4	4,1	7,2	11,5	17,6	21,6	24,6
60	23,4	16,5	11,6	5,9	2,3	0,9	1,5	4,1	8,6	15,4	20,4	24,6

ORIGINAL PAGE IS OF POOR QUALITY

The attenuation of the possible radiation by the cloud cover is determined as the function of the total amount of clouds and the midday height of the sun. The corresponding relations $f(n)$ are given in [20]. However it is difficult to use them when calculating the average values of the total radiation due to inadequate data regarding the frequency of each point for the clouds. There are only data regarding the average point of cloudiness for the water area of the oceans. Due to this Table 5 is proposed for

12

use in climatological calculations of radiation, which contains the value Q/Q_0 as a function of the average amount of total cloudiness (in points) obtained from data regarding the frequency of each point for the total amount of clouds [7].

TABLE 5. DEPENDENCE OF THE RATIO Q/Q_0 ON THE HEIGHT OF THE SUN AT MIDDAY h_M AND THE AVERAGE AMOUNT OF CLOUDS N (WITH ALLOWANCE FOR FREQUENCY).

h_M	n points										
	0	1	2	3	4	5	6	7	8	9	10
10°	1.00	1.02	1.01	0.97	0.92	0.84	0.76	0.67	0.58	0.49	0.37
20	1.00	1.02	1.01	0.97	0.92	0.84	0.76	0.67	0.56	0.47	0.35
30	1.00	1.01	0.99	0.97	0.92	0.84	0.77	0.68	0.58	0.49	0.37
40	1.00	1.00	0.99	0.96	0.92	0.85	0.78	0.70	0.60	0.51	0.40
50	1.00	1.00	0.98	0.95	0.93	0.85	0.79	0.71	0.62	0.54	0.42
60	1.00	1.00	0.98	0.95	0.93	0.85	0.79	0.73	0.61	0.55	0.44
70	1.00	0.99	0.97	0.95	0.93	0.85	0.80	0.74	0.65	0.56	0.46
80	1.00	0.98	0.96	0.94	0.93	0.86	0.80	0.74	0.67	0.58	0.48
90	1.00	0.96	0.95	0.94	0.92	0.87	0.82	0.76	0.69	0.61	0.50

The values of the midday heights of the sun on the average for each month are given in [33].

A table from the "Atlas of the Heat Balance of the Earth" was used to determine the albedo of the ocean surface [6]. These data closely coincide with the results of actinometric observations. The study [26] shows that the difference between both groups of data does not exceed 0.01, and in the majority of cases the values coincide.

The radiation of the atmosphere for a cloudless sky was determined as a function of the air temperature ϑ according to the formula

$$I_{a0} = 1.631 \sqrt{\vartheta^2 - 0.775}. \quad (8)$$

The influence of cloudiness upon the radiation of the atmosphere was considered by using the formula

$$I_a = I_0(1 + kn^2). \quad (9)$$

The empirical coefficient k in this formula is determined as a function of the air temperature θ (Table 6).

TABLE 6. VALUES OF THE COEFFICIENT k

θ	-20	-10	0	10	20	30
k	0.71	0.46	0.33	0.25	0.19	0.14

The coefficient β , which considers the difference between \bar{n}^2 and \bar{n}^2 was used in calculating the values of radiation (9). The factor β changes from 1.00 for a cloudiness of 0 and 10 points to 0.98 for a cloudiness of 3-6 points.

2.4. Loss of heat in evaporation from the surface of the land.

The loss of heat in evaporation is determined as a product of the latent heat of vaporation by the evaporation quantity. Since the latent heat of evaporation changes with a temperature change in the evaporating surface very slightly, a constant value of the specific heat of evaporation L , which equals 0.6 kcal/g was used in calculating the loss of heat to evaporation.

To calculate the monthly values of evaporation from land, a complex method was used based on the concurrent solution of the equations of heat and water balances and the experimentally established dependence of the evaporation rate on the soil humidity [15, 16, 17]. The following formulas were used in this method

$$E = E_0 \quad \text{at} \quad w \geq w_0. \quad (10)$$

$$E = E_0 \frac{w}{w_0} \quad \text{at} \quad w < w_0 \quad (11)$$

/13

where E and E_0 are the monthly sums of evaporation and evaporativity;

$w = \frac{w_1 + w_2}{2}$ - amount of productive moisture which is averaged over the month in the soil layer which is active for vegetation; w_1 and w_2 - amount of productive moisture at the beginning and end of the month; w_0 - critical value of the productive moisture of the soil above which the evaporation equals the evaporativity.

With the concurrent solution of equations (10) and (11) with the equation for the water balance

$$r = E + f + \Delta w \quad (12)$$

(r - rain; $\Delta w = w_2 - w_1$ change in the productive moisture. in the active soil layer where basically circulation occurs; f - discharge) the following formulas are obtained for determining the moisture:

$$w_2 = \frac{1}{1 + \frac{E_0}{2w_0}} \left[w_1 \left(1 - \frac{E_0}{2w_0} \right) + r - f \right] \quad (13)$$

for months when $w < w_0$.

$$w_2 = w_1 + r - f - E_0 \quad (14)$$

for months when $w \geq w_0$.

The formulas (10), (11), (13) and (14) make it possible to calculate the monthly values of the evaporation using the well-known monthly values of evaporativity, rain, and run-off.

When there is no information regarding the run-off, the formulas (15) and (16) may be used which establish the dependence of the run-off on the rain, evaporativity and moisture of the soil:

$$f = ar \frac{w}{w_h} \quad \text{at } r < E_0 \quad (15)$$

$$f = r \frac{w}{w_h} \sqrt{a^2 \left| 1 - \left(1 - \frac{E_0}{r} \right)^2 \right| + \left(1 - \frac{E_0}{r} \right)^2} \quad \text{at } r > E_0 \quad (16)$$

(w_k - productive moisture capacity, α - dimensionless proportionality coefficient which depends on the intensity of the rain and increases with an increase in their intensity).

The solution of equations (15) and (16) together with formulas (10) - (12) makes it possible to determine the monthly values of the productive moisture of the soil and then the moisture values of the evaporation and run-off using formulas (10 - 13). The yearly values of evaporation are found by summing the monthly values.

The layer of thickness of 1 meter is used as the active soil layer, since the basic mass of the roots of vegetation is concentrated in it and there is the greatest change in the moisture reserves with time. These changes are usually much less below a layer of a meter.

/14

The monthly values of the evaporativity E_0 may be calculated by the complex method [15, 16]. This method considers the basic factors which determine the evaporativity: radiation balance, temperature, and humidity of the air, turbulent exchange. The evaporativity E_0 is calculated by formula (17) which establishes the proportionality of evaporation from a moist surface to the deficit of the air humidity, determined from the temperature of the evaporating surface

$$E_0 = \rho D (e_s - e) \quad (17)$$

(E_0 - evaporativity; ρ - air density; D - integral coefficient of external diffusion; e_s - specific humidity of air saturated with water vapor at a surface temperature of θ_w ; e - specific humidity of the air).

The temperature of the surface θ_w is determined from the equation for the land heat balance under the condition of its adequate moisture

$$R = LE_0 + P + B \quad (18)$$

where the radiation balance $R = R_0 - 4\sigma\theta^4(\theta_w - \theta)$ (R_0 - radiation balance of the moist surface determined when calculating the effective radiation using the air temperature θ ; σ - coefficient characterizing the properties of the emitting surface), turbulent heat flux $P = \rho c_p D(\theta_w - \theta)$ (c_p - heat capacity of the air; B - heat flux between the land surface and the underlying layers; L - latent heat of evaporation). Calculating the radiation balance R_0 and the heat flux in the soil B [16], and knowing θ and e from meteorological observations, using the equation of heat balance we may determine the values of the quantities θ_w and e_s which are interrelated by the empirical formulas for the dependence of the elasticity of the saturated water vapor on temperature (the Magnus formula). The evaporativity calculations were performed for the monthly time intervals. After determining e_s , and using formula (17) the monthly values of E_0 are found. The yearly value of evaporativity is determined by summing the monthly values. The coefficient of external diffusion D is assumed to equal 0.63 cm/sec in the calculations [15]. Estimates show that the influence of a change in the coefficient D on evaporativity is small [15, 31].

Using the method examined, when compiling the "Atlas of the Heat Balance of the Earth" [6] the yearly and monthly values of evaporativity, and the yearly and monthly maps of evaporativity for Earth were drawn up based upon them [24]. During this investigation, the values for the humidity deficit, determined from the average monthly values for the temperature and the air humidity, were refined by introducing a correction caused by a nonlinear characteristic of the dependence of the saturated water vapor elasticity upon temperature (Ol'dekop correction). This correction may amount to 2 - 3 mm/month. In moist regions it is small and as a rule amounts to fractions of millimeters per month. Allowance for this correction led to an increase in the monthly and yearly values of evaporativity which in certain regions amounted to 5% for the year and 10% for certain months.

The refined values of the radiation balance were used in evaporativity calculations [1, 3, 30]. The evaporativity values increased up to 20% in certain moist equatorial regions due to this refinement, as compared with the preceding values [24].

The values of the critical humidity which are necessary for the calculations were determined by processing these materials on the water balance of the soil. Depending on the geographical conditions and the time of year, the average rounded off values of w_0 for the upper meter layer of the soil changed basically from 100 to 300 millimeters per month [31].

Using data on the discharge, the proportionality coefficient α in formulas for establishing the discharge (15) and (16) was determined by region. The value of α was found to equal 0.2 for territories to the north of 45° north latitudes for deserts, tropical semi-deserts and for dry savannas. For regions with abundant rain, the coefficient α equals 0.6; for the remaining territory it is close to 0.4 [31].

In the calculations the values of the productive soil moisture capacity of w_k was assumed to equal 200 meters per meter layer of soil (average value of the smallest soil moisture capacity), with the exception of certain regions of excessive moisture where $w_k = 350$ was used in the calculations (a value close to the average total soil moisture capacity).

The calculations of the soil moisture were performed for the entire period with a great change in the moisture of the soil meter layer. Basically this period coincides with a period of positive air temperatures. The equations for determining the soil moisture for all of the months with positive temperatures were solved by the method of successive approximation [16, 17, 31].

In calculations of soil moisture for territories with high positive air temperatures, throughout the entire year, it was

advantageous to begin the calculations from the end of the rainy period. In this case it may be assumed that the quantity w_1 is close to w_0 .

After determining the average monthly values of the soil moisture, the monthly values of evaporation were found using equations (10) and (11).

A criterion for the validity of these calculations is the satisfaction of the water balance equation ($r = E + I$ for the year and $r = E + I + w_2 - w_1$ for months)..

In the method examined the values of w_0 are used which are averaged in the limits of large territories. The estimates made for different climatic conditions showed that the change in w_0 in a very wide interval leads to a comparatively small change in the ratio w/w_0 and the monthly values of evaporation connected with them.

An analysis of the materials on the dynamics of soil moisture [18] is at the basis of the assumption assumed in the calculation for the constant soil moisture throughout the winter period. This showed that the movement of moisture to the surface, which occurs when the soil is frozen, is considerable for average conditions in regions of excess and adequate moisture. Since under these conditions the evaporation is close to the evaporativity, allowance for the auxiliary moisture does not have a great influence upon the evaporation calculations. The penetration into the soil of water during a thaw as a rule does not change the moisture balance of the meter layer, or changes it insignificantly.

It is very complex to determine the accuracy of the evaporation calculations since not one of the existing methods for determining evaporation can be assumed to be a reference method. Thus,

to determine the reliability of evaporation calculations by the methods considered, a comparison was made of the calculated monthly and yearly values of evaporation with the values determined by other independent methods -- the method of heat balance [10,34], water balance and the method of determining the evaporation by evaporators [17, 29, 31]. These comparisons showed that all of the methods examined (except for the method of evaporators which was used in a zone of inadequate moisture) agreed satisfactorily between each other. Thus, the accuracy of the results from using the complex method was comparable with the accuracy of the methods of heat and water balance, and in some cases had an advantage over the method of determining evaporation by means of evaporators [31]. The turbulent heat flux between the land surface and the atmosphere P was determined as the residual term of the heat balance equation. For the yearly period P was assumed to equal the difference between the radiation balance and the heat loss to evaporation. For shorter periods, apart from the heat loss to evaporation, it is necessary to subtract the heat flux into the soil during this period from the radiation balance.

2.5. Heat loss to evaporation from the ocean surface and turbulent heat exchange between the ocean surface and the atmosphere.

To determine the turbulent heat fluxes P and the moisture E above the oceans, a computational method was used [2], based on the following formulas

$$P = \rho c_p \alpha u \Delta \theta, \quad (19)$$

$$E = \frac{0.622 \rho}{p} c_e u \Delta \theta, \quad (20)$$

where ρ - air density; c_p - specific heat capacity of the air;
 α - heat exchange coefficient; u - wind velocity; $\Delta \theta$ - temp- /17

erature difference (water - air); p - atmospheric pressure; c_k - coefficient of moisture exchange; Δc - difference between moisture of air saturated by water vapor at the level of the water surface and the air moisture at the height of ship observations.

It is apparent that the second of these formulas is similar to formula (17).

The values of the heat and moisture exchange coefficients, which were assumed to be equal, were found by means of the nomograms [13] as a function of the wind velocity and the stratification of the latter layer characterized by data on the difference between the effective temperatures of the water and air $\Delta\theta_{ef} = \Delta\theta + 0.106\Delta c$. These values were determined for the observational conditions in specific time periods.

Corrections were introduced for the values of the heat exchange coefficient C_0 in the calculation of the fluxes P and E , determined from the average monthly data of ship's observations, due to fluctuations in u , $\Delta\theta$ and Δc . The expressions for the calculation of the heat and moisture fluxes in these cases have the form

$$P = \rho c_p \left\{ c_0(u, \Delta\theta_{ef}) + \frac{\partial c_0}{\partial u} \frac{\sigma_u^2}{u} + \frac{\partial c_0}{\partial (\Delta\theta_{ef})} \left(1 + \frac{0.07}{Bo} \right) \frac{\sigma_{\Delta\theta}^2}{\Delta\theta} \right\} \bar{u} \Delta\bar{\theta} \quad (21)$$

$$E = \frac{0.622p}{p} \left\{ c_E(\bar{u}, \Delta\bar{\theta}_{ef}) + \frac{\partial c_E}{\partial u} \frac{\sigma_u^2}{u} + \frac{\partial c_E}{\partial (\Delta\bar{\theta}_{ef})} \times \right. \\ \left. \times \left(0.106 + \frac{Bo}{0.66} \right) \frac{\sigma_{\Delta c}^2}{\Delta c} \right\} \bar{u} \Delta\bar{c}, \quad (22)$$

where Bo is the Bouen relationship, which equals $0.66 \frac{\Delta\theta}{\Delta c}$; σ_u^2 - dispersion of the wind velocity; $\sigma_{\Delta\theta}^2$ - dispersion of the temperature difference; $\sigma_{\Delta c}^2$ - dispersion of the moisture difference.

The study [2] gives the values of the first derivatives of the parameter c_0 for the wind velocity and the temperature drop and also the empirical values of the dimensionless dispersions $\frac{\sigma_u^2}{u^2}$, $\frac{\sigma_{\Delta\theta}^2}{\Delta\theta^2}$ and $\frac{\sigma_{\Delta c}^2}{\Delta c^2}$. These values are necessary for intro-

ducing corrections to the heat and moisture exchange coefficient.

Expressions (21) and (22) describe the heat and moisture exchange of the ocean surface with the atmosphere for low and average wind velocity.

In the case of storm winds, the coefficients of heat and moisture exchange greatly increase. To take into account the influence of storms upon the average monthly values of the heat and vapor fluxes, use was made of the dependence of the coefficient c on the wind velocity in the interval from 15 to 33 meters per second [14]. Taking into consideration the distribution of the probabilities of the storm wind velocity for different values of the wind velocity which was averaged over the month, the effective values were obtained for the coefficient c_p^* for 3 gradations of the storm wind: 17-21 meters/second (8 point), 21-24 meters/second (9 points) and 24-30 meters/second (10-11 points) as a function of the average velocity [2].

Taking into account the influence of stratification of the air layer and storms, the turbulent fluxes of heat and moisture over a monthly time interval were calculated using the average values of the initial quantities of $(\bar{u}, \Delta\bar{\theta}, \Delta\bar{e})$ by means of the formulas

$$\begin{aligned}
 P = A \left\{ [1 - q(u \geq 17)] \left[c_p(\bar{u}, \Delta\bar{\theta}_{sp}) + \frac{\partial c_p}{\partial u} \frac{\sigma_u^2}{\bar{u}} + \right. \right. \\
 \left. \left. + \frac{\partial c_p}{\partial (\Delta\bar{\theta}_{sp})} \left(1 + \frac{0.07}{150} \right) \frac{\sigma_{\Delta\bar{\theta}}^2}{\Delta\bar{\theta}} \right] \bar{u} \Delta\bar{\theta} \cdot 10^2 + \right. \\
 \left. + (q(17-21)c_p^*[(17-21), \bar{u}] \cdot 19.0 + q(21-24)c_p^* \times \right. \\
 \left. \times [(21-24), \bar{u}] \cdot 22.5 + q(24-30)c_p^*[(24-30), \bar{u}] \cdot 27.0) \times \right. \\
 \left. \times 10^2 \Delta\bar{\theta} \right\} \text{ kcal}/(\text{cm}^2 \cdot \text{month}) \quad (23)
 \end{aligned}$$

$$\begin{aligned}
 E = B \left\{ [1 - q(u \geq 17)] \left[c_E(\bar{u}, \Delta\bar{\theta}_{sp}) + \frac{\partial c_E}{\partial u} \frac{\sigma_u^2}{\bar{u}} + \right. \right. \\
 \left. \left. + \frac{\partial c_E}{\partial (\Delta\bar{\theta}_{sp})} \left(0.106 + \frac{B_0}{0.66} \right) \frac{\sigma_{\Delta\bar{\theta}}^2}{\Delta\bar{\theta}} \right] \bar{u} \Delta\bar{e} \cdot 10^2 + \right. \\
 \left. + (q(17-21)c_E^*[(17-21), \bar{u}] \cdot 19.0 + q(21-24)c_E^* \times \right. \\
 \left. \times [(21-24), \bar{u}] \cdot 22.5 + q(24-30)c_E^*[(24-30), \bar{u}] \cdot 27.0) \times \right. \\
 \left. \times 10^2 \Delta\bar{e} \right\} \text{ cm/month} \quad (24)
 \end{aligned}$$

In formulas (23 and 24) the quantity $q(u \geq 17) = q(17-21) + q(21-24) + q(24-30)$ designates the probability of the wind velocity exceeding 17 meters/second [2]. The numerical coefficients A and B are equal (upon substituting u in meters/sec. into the formula $\Delta \theta$ in °C, Δe in mbar, and a month duration of 30 days $A=0,794$; $B=2,057$).

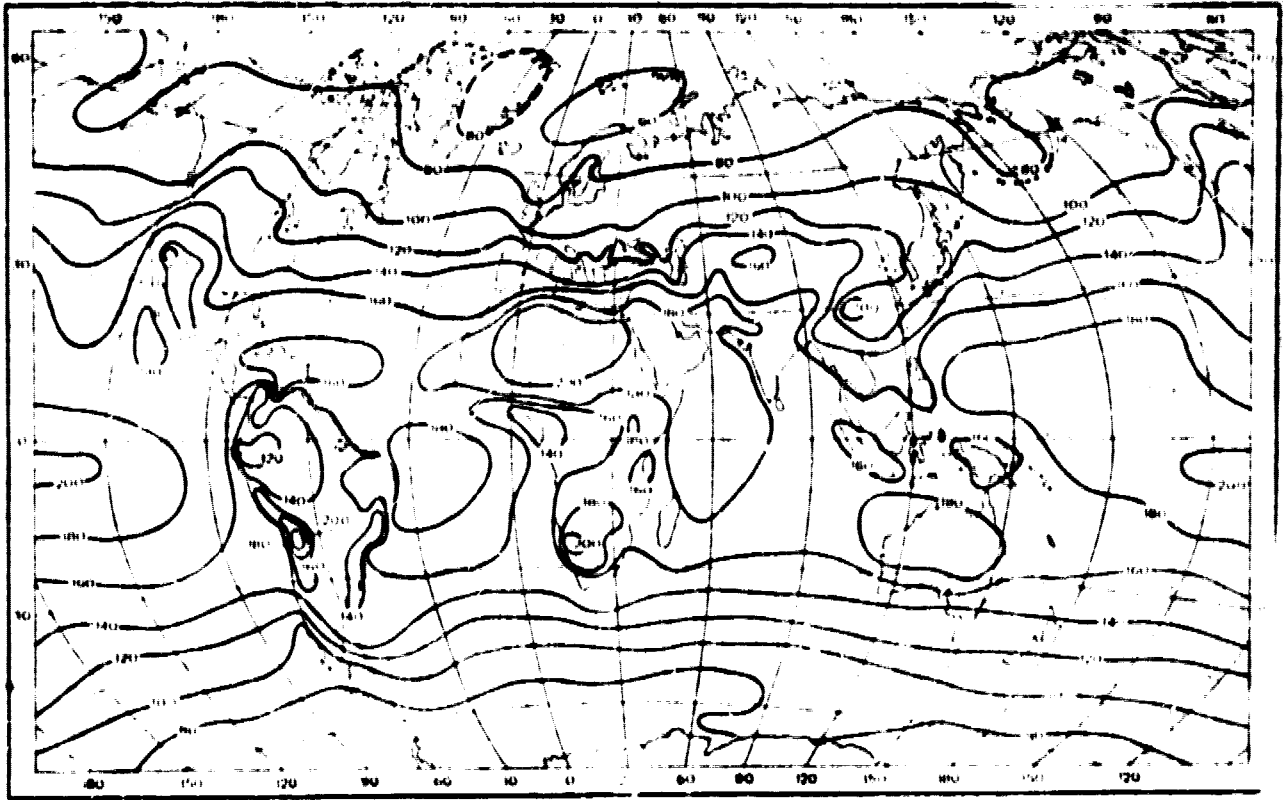
The heat loss to evaporation from the ocean surface was determined as LE, where $L = (597 - 0,56Q_e) \cdot 10^{-3}$ cal/year.

3. World Maps for the Heat Balance Components

3.1. Total radiation

As may be seen from figure 1, the yearly values of the total radiation on the Earth change from values of ≤ 40 to ≥ 200 kcal/(cm² · yr.). The largest values both on the land and on the ocean are confined to the belts of high pressure in the northern and southern hemispheres. The values of the total radiation decrease in the direction toward the high latitude. A certain decrease in the values examined is also characteristic for the equatorial latitudes, which is connected to the great frequency of cloudiness throughout the entire year.

The distribution of the isolines of the total solar radiation has basically a zonal nature which is greatly disturbed by the non-uniform distribution of cloudiness. The zonality disturbances occur in the following regions: 1) in the moderate latitudes of both hemispheres, where cyclone activity is greatly developed (the western coast of Canada and North Europe, southwest coast of South America); 2) in the eastern regions of the tropical zones of the ocean under the influence of inversions and cold sea currents; 3) in the region of monsoons (Indonesia, eastern coast of Asia, northwest Indian Ocean).



ORIGINAL FIGURE
OF 1950

Figure 1. Total solar radiation ($\text{kcal}/(\text{cm}^2 \cdot \text{yr})$), yearly.

In an examination of data on the distribution of the total radiation for the winter months, one notes that there is a rapid decrease in the direction toward the poles of the corresponding hemispheres which is related to a reduced reduction in the midday height of the Sun and a shortened day. In addition to this, for the winter large interlatitudinal changes in the radiation sums are characteristic; from values of about $14 \text{ kcal/cm}^2 \cdot \text{month}$ at the low latitudes to values which equal zero in the polar circle where the solar radiation does not enter.

The largest monthly sums of solar radiation at the low latitudes occur in the regions of the oceans and the regions of equatorial monsoons on the continents where there is little cloudiness during this time.

Distinguishing features of the summer distribution of the total radiation are the high values of this radiation throughout the entire hemisphere with a small geographic change.

The tropical and sub-tropical deserts receive the maximum amount of solar heat (above $20 \text{ kcal}/(\text{cm}^2 \cdot \text{month})$). A large amount of solar energy in the summer also reaches the polar regions, where the influence of the low heights of the sun is compensated by very long days. The greatest values of solar radiation are in the summer months in the central plateau of Antarctica. Thus, in January the monthly sums change from $16-18 \text{ kcal/cm}^2$ on the coast to 30 kcal/cm^2 inside the continent, which greatly exceeds the value for the region of the tropical deserts.

For a large portion of the surface of the continents, the data given in figure 1 closely coincides with the similar map of the "Atlas of the Heat Balance of the Earth." Certain changes must be noted for regions located in the tropical and equatorial latitudes. Thus in regions of the tropical deserts, the radiation is somewhat diminished and in the equatorial regions it increases [11, 12].

On the oceans the total radiation has increased everywhere by 13% on the average. This increase in the total radiation is due to the use of a new method for determining the components of the radiation balance of the ocean surfaces.

The data in Table 7 show these differences. It gives the zonal distribution of the yearly values of total solar radiation calculated from data in the "Atlas of the Heat Balance of the Earth" [6] (1963), and the present study [1975] using materials on the Arctic Ocean from the monograph [30]. It follows from this that the changes obtained in solar radiation for individual latitudinal zones of the Earth did not indicate the average values for the Earth as a whole, which equalled $138 \text{ kcal}/(\text{cm}^2 \cdot \text{year})$. For the oceans, the latter quantity increased, which increased the average yearly value Q for the entire surface of the Earth by 9%.

The difference in the maps of total radiation mentioned above do not change the general character of its distribution on the surface of the Earth. Thus, new results may be regarded as corroborating the conclusions regarding the patterns in the distribution of solar radiation given in the "Atlas of the Heat Balance of the Earth."

/22

TABLE 7. LATITUDINAL DISTRIBUTION OF THE YEARLY VALUE OF THE TOTAL SOLAR RADIATION (KCAL/(CM²))

Latitudinal zone	Land		Ocean		Surface of the Earth	
	1963	1978	1963	1973	1963	1973
90-80° N		76		70		71
80-70		78		70		73
70-60	79	84	69	75	76	82
60-50	94	100	68	90	83	96
50-40	124	127	90	113	108	121
40-30	162	155	126	142	141	148
30-20	192	175	156	168	170	171
20-10	174	181	164	177	167	178
10-0	144	158	157	177	154	173
0-10° S	145	150	160	181	156	174
10-20	167	165	160	177	162	174
20-30	178	173	149	165	156	166
30-40	154	161	128	144	131	145
40-50	110	122	93	116	94	116
50-60	84	86	67	87	67	87
60-70		97		74		77
70-80		99		77		92
80-90		98				98
Earth as a whole	138	138	127	144	130	142

3.2. Radiation Balance

The yearly sums of the radiation balance of the surface of the Earth change from values which are less than 5 kcal/cm² in the Antarctic and close to zero in the central regions of the Arctic, up to 90-95 kcal/cm² in the tropical latitudes.

The influence of astronomical factors causes the zonal distribution of the yearly and monthly sums of the radiation balance in flat territories located at the high and middle latitudes of the northern hemisphere. The latitudinal distribution is disturbed in regions where the circulation factors greatly change the cloudiness conditions as compared with the average values.

The geographic zones of the high and middle latitudes are characterized by definite yearly sums of the radiation balance: the arctic tundra - less than 10 kcal/(cm² · year); the tundra, forest tundra 10-20 kcal/(cm² · year); the northern and middle taiga 20-30 kcal/(cm² · year); the southern taiga 30-35 kcal/(cm² · yr); mixed leafy broad-leaved forests, the forest steppes

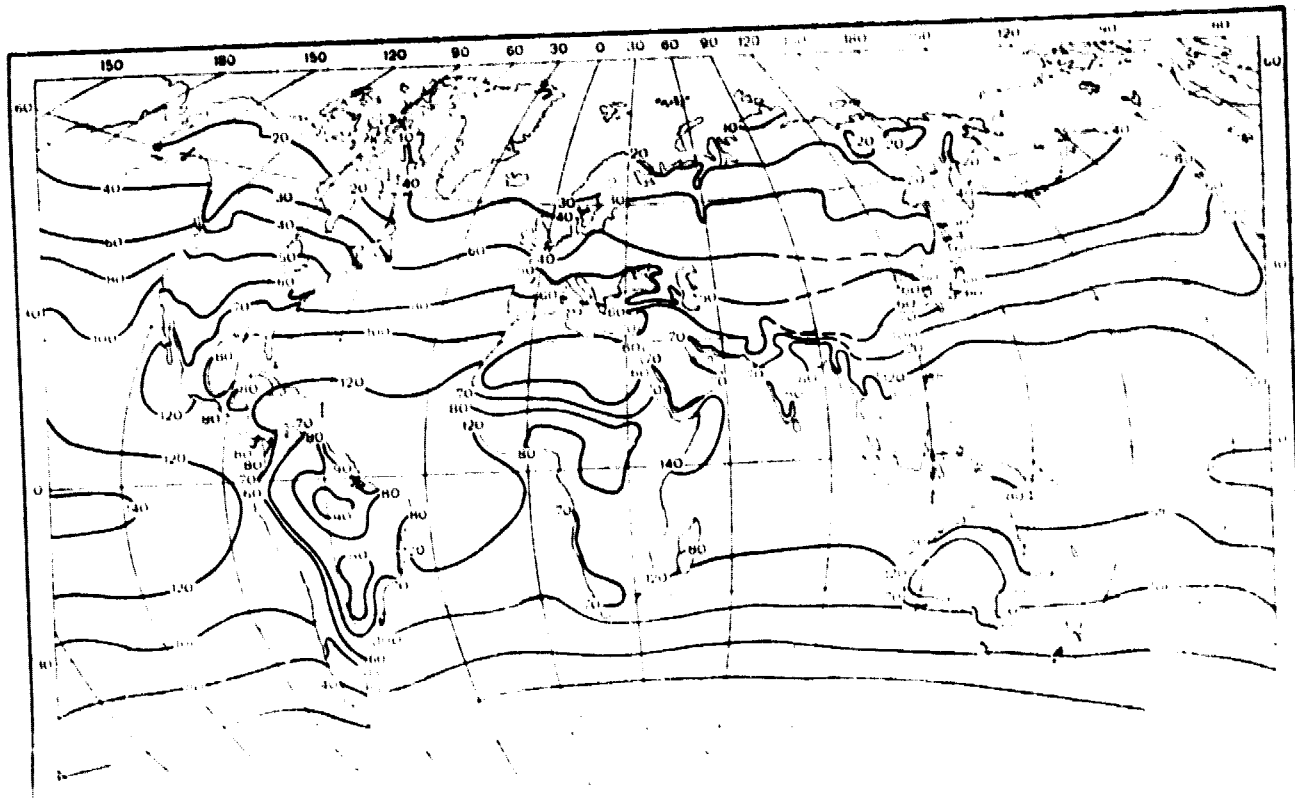


Figure 2.

and steppes of the moderate latitudes, 35-50 kcal/(cm² · year) (figure 2).

In the subtropical, tropical and equatorial zones, the characteristics of atmospheric circulation produce sharp differences in the clouds and moisture conditions, due to which the yearly values of the radiation balance change in the zones from 55 to 95 kcal/cm². Thus the minimum values of the radiation balance are confined to the regions of subtropical and tropical deserts and are due to the great reflectivity of the surface of the deserts and the great heat losses due to long wave radiation under conditions of clear weather, dry air, and the high temperature of the soil surface.

It follows from the data on the distribution of the radiation balance in individual months that the smallest values of the radiation balance in winter and in summer occur at the high polar latitudes (from -1 to -2 kcal/(cm² · month) in winter and about 4 kcal/(cm² · month) in summer. At the moderate latitude of the northern hemisphere, there are very uniform fields of the radiation balance from -1 to -2 kcal/(cm² · month) in January and from 7 to 9 kcal/(cm² · month) in July. In the tropical and equatorial latitudes, during the winter solstice the value of the radiation balance decreased to 3.5-4.0 kcal/(cm² · month), and in the summer months the maximum values reached 9-10 kcal/ /24 (cm² · month), and decreased to 5.5 - 6.0 kcal/cm² in the regions of deserts and equatorial monsoons.

As compared with data on the radiation balance of the surface of the Earth given in the "Atlas of the Heat Balance of the Earth" [6], the yearly sum of the radiation balance shown in Fig. 2. decreased by 10-15% in several tropical regions (the northern part of Indonesia, the Sahara, etc) and increased by 10-20% in the zone of humid equatorial forests and by 5-15% in the steppe and forest steppe zone of the moderate latitudes. These changes

are related to the use of new materials in observations of the total radiation, a decrease in the albedo used for the humid tropical forests, and a decrease in the effective radiation due to the increased heat losses to evaporation. However, for individual latitude zones and the Earth as a whole the values of the radiation balance changed comparatively little (Table 8).

TABLE 8. AVERAGE LATITUDINAL VALUES OF THE RADIATION BALANCE (kcal/(cm² · year)

Latitudinal zone	Land		Oceans	
	1963	1975	1963	1975
70-60° N	20	22	23	23
60-50	30	32	29	43
50-40	45	45	51	64
40-30	60	58	83	90
30-20	69	64	113	111
20-10	71	74	119	121
10-0	72	79	115	124
0-10° S	72	79	115	127
10-20	73	75	113	122
20-30	70	71	101	109
30-40	62	62	82	92
40-50	41	44	57	72
50-60	31	35	28	46
Earth as a whole	49	50	82	91

The distribution of the values of the radiation balance on the surface of the oceans, shown on the maps, is similar to the distribution of the total radiation. The maximum value of the radiation balance on the oceans exceeds 140 kcal/(cm² · year). The minimum for the surface of the oceans which is free of ice is located on the boundary of the floating ice - about 20-30 kcal/(cm² · year). It must be noted that the yearly sums of the radiation balance are positive over all the areas of the oceans.

In the winter months the radiation balance changes in terms of latitude from 8-10 kcal/(cm² · month) in the equatorial and tropical latitudes up to small negative values at the high latitudes (about -4 kcal/(cm² · month). Thus in January the radiation balance is negative in both hemispheres above 45° north and southern latitudes.

In the summer months the values of the radiation balance reach a maximum (more than $14 \text{ kcal}/(\text{cm}^2 \cdot \text{month})$) in the tropical latitude, descending to $8-9 \text{ kcal}/(\text{cm}^2 \cdot \text{month})$ at the high latitudes. In these months the distributions of the radiation balance, in contrast to the winter, deviate greatly from the zonal distributions and the region of high and low values correspond to regions of high and low cloudiness.

As compared with the results of calculations shown in the "Atlas of the Heat Balance of the Earth" [6], new data on the radiation balance of the ocean (Table 8) is higher in both hemispheres by 11% on the average, which is due to an increase in the total radiation.

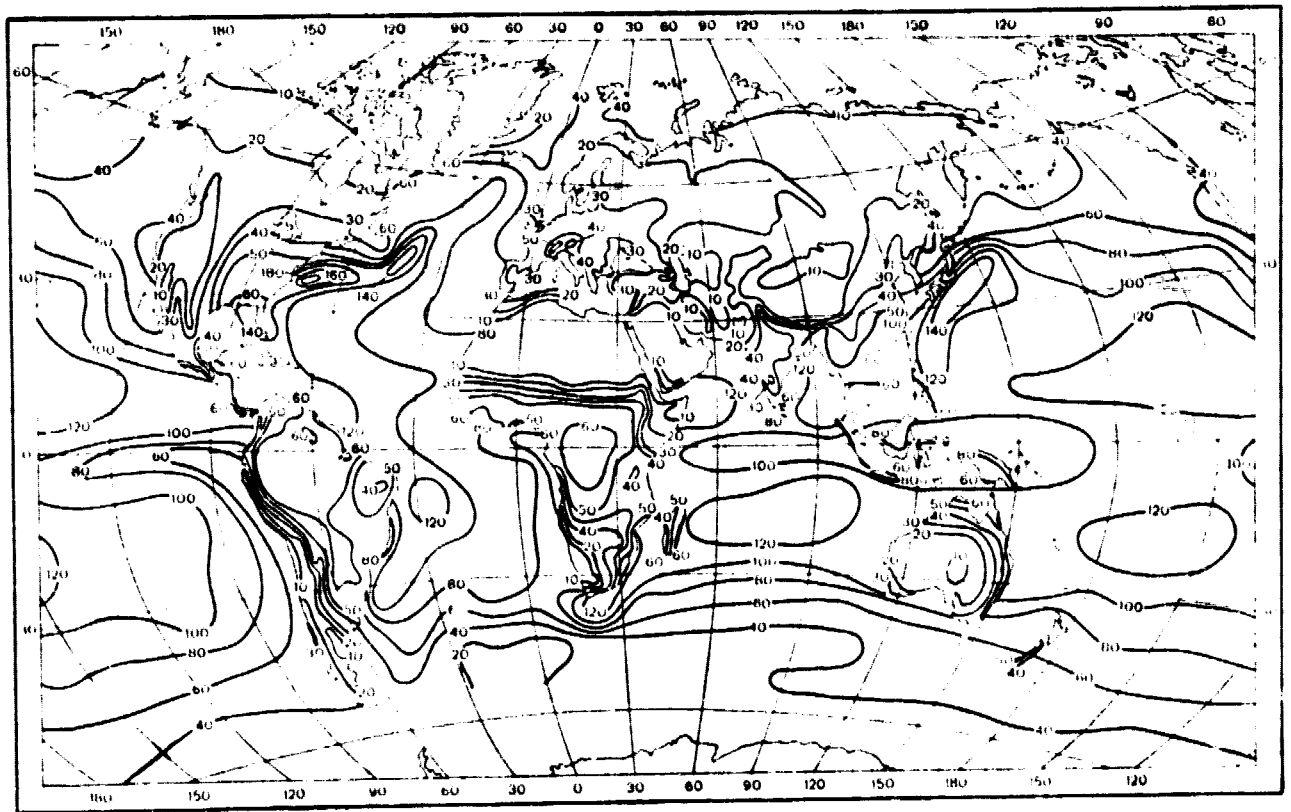
For the Earth as a whole, the radiation balance of the Earth's surface increased by 10%.

3.3. Heat Loss to Evaporation

The yearly map of heat loss to evaporation is shown in Figure 3. The distribution of the values for heat loss to evaporation for the Earth is based on calculations by a complex method of the average multi-year, monthly values of evaporation for 1700 points located on flat areas. For the mountainous regions of the Earth, the heat loss to evaporation was estimated on the basis of data regarding the vertical evaporation gradient [31].

The average monthly values of heat loss to evaporation (and turbulent heat exchange with the atmosphere) on the oceans was calculated for 722 points. The initial material for the calculation was the data from the sea climatic atlas [51] and also data from multi-year ship observations in 10-degree squares on the Atlantic, Indian and Pacific Oceans [4].

Considering the features of the distribution for the heat



REPRODUCED FROM
JOURNAL OF CLIMATE

Figure 3. Heat loss to evaporation ($\text{kcal}/(\text{cm}^2 \cdot \text{year})$). Yearly.

loss to evaporation on land, it may be noted that the range in its change of values is about $80 \text{ kcal}/(\text{cm}^2 \cdot \text{year})$. In regions of high moisture, the heat loss to evaporation increases together with an increase in the radiation balance from the high latitudes to the equator, changing from values which are less than $10 \text{ kcal}/(\text{cm}^2 \cdot \text{year})$ on the northern coast of the continent, to $70-80 \text{ kcal}/(\text{cm}^2 \cdot \text{year})$ and the humid equatorial forests of South America, Africa, and the Malay archipelago. In regions of low humidity, the heat loss to evaporation is determined by the dryness of the climate, decreasing with an increase in the dryness. The smallest values of heat loss to evaporation are noted in the tropical deserts, where they are about several $\text{kcal}/(\text{cm}^2 \cdot \text{year})$ in all. /27

The yearly pattern of heat loss to evaporation is also determined by the reserve of heat and moisture. At the extra-tropical latitudes with conditions of high humidity, the greatest values of heat loss to evaporation are found in summer in accordance with the yearly pattern of the radiation balance reaching $5-6 \text{ kcal}/(\text{cm}^2 \cdot \text{month})$. In winter the heat loss to evaporation is low. In regions of low humidity, the maximum heat loss to evaporation moves within the thermal period as a function of the humidity conditions. In the desert, the yearly pattern LE is determined by the yearly pattern of the precipitation.

At the tropical latitudes with a humid climate, the heat loss to evaporation is great throughout the year and is about $6-8 \text{ kcal}/(\text{cm}^2 \cdot \text{month})$. In regions with seasons of low precipitation there is a certain decrease in the heat loss to evaporation. However, its amplitude of the yearly pattern is comparatively small. In regions with a clearly pronounced dry period, the greatest values for heat loss to evaporation are found at the end of the rainy period and the smallest are found at the end of the dry period.

On the whole for the Earth (including Antarctica) the heat loss to evaporation is $27 \text{ kcal}/(\text{cm}^2 \cdot \text{year})$. The average latitudinal values for land are given in Table 9 which compares data from present calculations with values obtained in previous calculations. It may be seen from the table that the greatest divergence between the previous and new values of the heat loss to evaporation is observed at the pre-equatorial latitudes.

TABLE 9. AVERAGE LATITUDINAL VALUES OF HEAT LOSS TO EVAPORATION. ($\text{KCAL}/(\text{CM}^2 \cdot \text{YEAR})$)

Latitudinal zone	Land		Oceans	
	1963	1973	1963	1973
70-60° N	14	16	33	31
60-50	19	23	39	47
50-40	24	25	53	67
40-30	23	23	86	96
30-20	20	19	105	109
20-10	29	32	99	117
10-0	48	57	80	104
0-10° S	50	61	84	99
10-20	41	45	104	113
20-30	28	28	100	106
30-40	28	29	80	82
40-50	21	22	55	51
50-60	20	22	31	35
Earth as a whole	25	27	74	82

The values obtained in this study for these latitudes are above the previous ones (by 15% at the Equator) basically due to the refinement of the radiation balance for the pre-equatorial latitudes. For the remaining latitudes the differences between the heat loss to evaporation are small and, as a rule, are due to refinements of the amount of precipitation. As may be seen, the laws governing the latitudinal distribution of heat loss to evaporation on land remain the same as previously.

A comparison of the values for heat loss to evaporation and radiation balance shows that during the year as a whole

for the surface of the land, 55% of the radiation balance is lost to evaporation. The remaining 45% is lost to turbulent heat exchange between the Earth's surface and the atmosphere. Thus in regions of excessive humidity from 70 to 90% of the radiation balance is lost to evaporation. In deserts the loss of radiation balance to evaporation is small.

The distribution of the yearly values of heat loss to evaporation on the oceans in general is similar to the distribution of the radiation balance. As may be seen from the map (Figure 3), the change in the heat loss to evaporation is rather great: from values close to $120 \text{ kcal}/(\text{cm}^2 \cdot \text{year})$ at the tropical latitudes to values of about $30 \text{ kcal}/(\text{cm}^2 \cdot \text{year})$ at the boundary of the icebergs. At the equatorial latitudes the heat loss to evaporation is somewhat lower than the higher latitudes (less than $100 \text{ kcal}/(\text{cm}^2 \cdot \text{year})$), which is due to an increase in cloudiness and humidity.

In addition to the radiation heat, heat which is transferred by currents is also lost to evaporation from the ocean. Therefore the zonal nature of the distribution of heat loss to evaporation is disturbed by great deviations in the regions of hot and cold currents. This may be clearly seen on the map shown in this article. The greatest heat loss to evaporation takes place in the northern hemisphere: more than $180 \text{ kcal}/(\text{cm}^2 \cdot \text{yr.})$ year) in the region of the Gulf Stream and about $140 \text{ kcal}/$ in the Curacao region, where the air humidity deficit is higher not only due to a high water temperature but also due to comparatively low humidity of the air entering these regions from the continents of North America and Asia during the cold time of the year.

The yearly sums of heat loss to evaporation may be compiled basically from values in the autumn-winter period.

The distribution of heat loss to evaporation in the winter

months is similar to the yearly distribution. During this time there is an increase in the influence of the thermal currents, due to which the characteristics of individual oceans is clearly expressed: heat loss to evaporation from the surface of the North Atlantic at the moderate latitudes is twice as large as at the latitudes of the Pacific Ocean. The lowest values of heat loss to evaporation are noted at the moderate latitude of the southern hemisphere in the Atlantic and Indian Oceans. In these regions with comparatively low water temperatures, warmer air masses enter from the low latitudes, which decreases the heat loss to evaporation.

/29

With the change to summer, the influence of the warm currents upon the magnitude of the heat loss to evaporation is reduced, due to a decrease in the energy reserves of the current. Since in the summer months there is a reduction of the average wind velocities and a reduction in the contrast between the temperature of water and air, the heat loss to evaporation greatly decreases. In addition, there is a decrease in the difference in the values of heat loss to evaporation from the surface of individual oceans.

When comparing the yearly map of heat loss to evaporation from the surface of the world's ocean with the similar map given in "Atlas of the Heat Balance of the Earth" [6], we may note that the general geographic laws governing the distribution of heat loss to evaporation from the surface of the oceans is the same as before. This may be seen from Table 9.

It may be seen that on a large section of the world's ocean the new values for heat loss to evaporation are higher than the values obtained previously. There is a particularly large increase in the heat loss to evaporation at the low latitudes which is due to the use of a new method in the calculations, which considers the increase in the evaporation

coefficient when there are large deficits of air humidity and weak winds which are characteristic for these latitudes.

On the average the heat loss to evaporation from the surface of the world's oceans increased by 11%.

3.4. Turbulent Heat Flux Between the Earth's Surface and the Atmosphere.

Figure 4 shows a map of the turbulent heat flux for the year.

The largest value of the turbulent heat flux between the land surface and the atmosphere is noted in the tropical deserts where they reach $55-60 \text{ kcal}/(\text{cm}^2 \cdot \text{year})$. With an increase in the humidity of the climate, the turbulent flux decreases. Thus in regions of humid tropical forests the turbulent flux is $10-20 \text{ kcal}/(\text{cm}^2 \cdot \text{year})$. Moving to the higher latitudes, the turbulent flux decreases together with a decrease in the radiation balance. On the northern coasts of the continents of the northern hemisphere, the turbulent flux is less than $5 \text{ kcal}/(\text{cm}^2 \cdot \text{year})$. The same values are noted for regions of high humidity at the moderate latitudes.

The same uniformity is observed in the yearly pattern - an increase in the turbulent flux with an increase in the radiation balance. In view of this, at the extratropical latitudes the largest yearly values of the turbulent flux are found in summer - and the smallest ones in winter. Thus for areas located above 40° north and south latitudes, there is a characteristic displacement of the direction of the turbulent flux throughout the year. In winter the Earth's surface receives heat from the atmosphere by turbulent heat exchange. However, the values of the heat transfer by the atmosphere are small, even in the extreme north they are less than $1 \text{ kcal}/(\text{cm}^2 \cdot \text{month})$.

ORIGINAL PAGE IS
OF POOR QUALITY

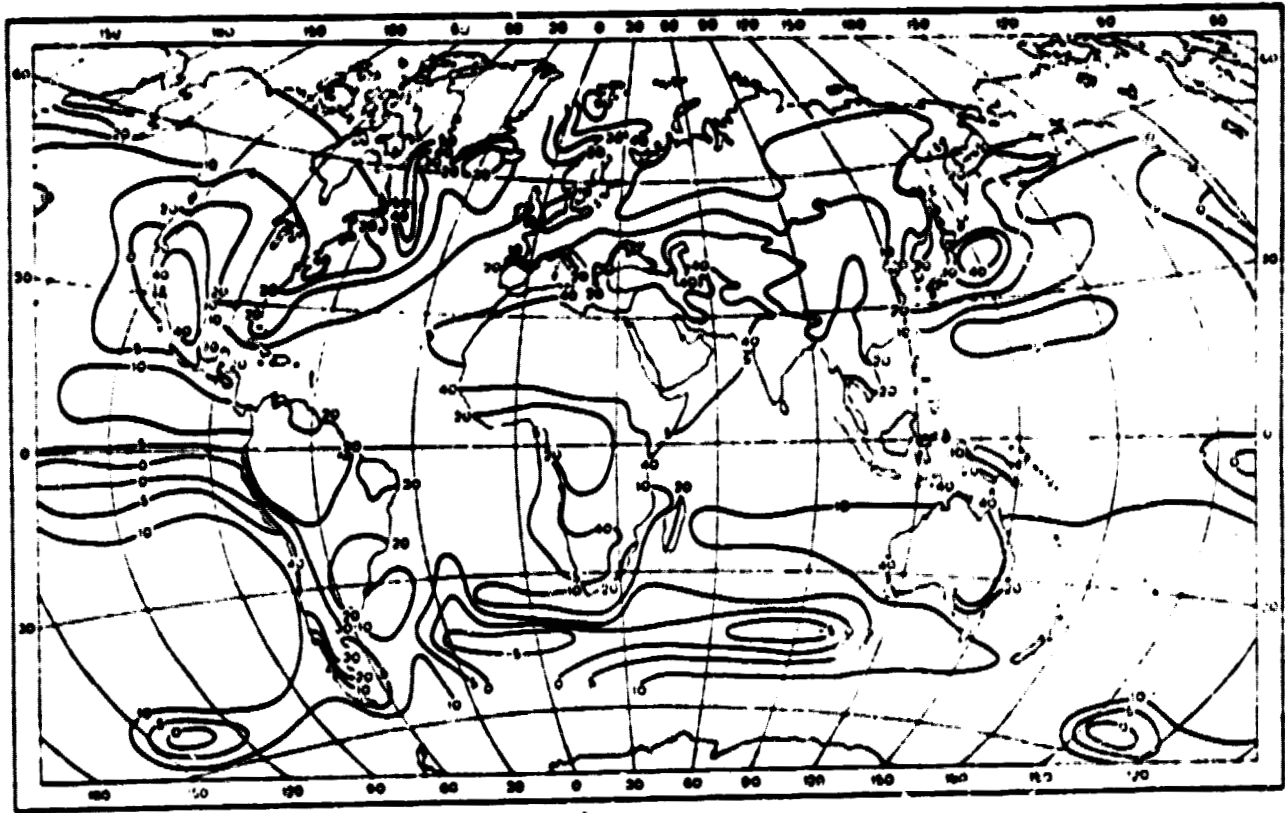


Figure 4. Turbulent heat flux from the Earth's surface to the atmosphere ($\text{kcal}/(\text{cm}^2 \cdot \text{year})$). Yearly. (The heat flux is positive when it is directed from the Earth's surface to the atmosphere).

The surface of the continents from the equator to 40° north and south latitudes throughout the entire year releases heat by turbulent heat conductivity. Thus at the low latitudes the yearly pattern of the turbulent flux greatly depends on the humidity. The largest monthly values of the turbulent flux are observed during the minimum of atmospheric precipitation. At the subtropical latitudes with a mediterranean type of climate the maximum values of the turbulent flux are observed in summer and amount to 6 kcal/(cm² · month). In the deserts, particularly the coastal deserts, where the processes of the transformation of the air masses at the water-land boundary have a great influence upon the turbulent heat exchange, the values of the turbulent flux exceeds 6 kcal/(cm² · month). In the humid tropical regions the turbulent flux is small throughout the entire year, and its monthly values are less than 2 kcal/cm².

On the whole, 45% of the yearly value of the radiation balance of the surface of the continents is expended on turbulent heat exchange with the atmosphere throughout the year.

A map of the turbulent heat exchange of the surface of the oceans with the atmosphere shows that almost everywhere there is heat loss by the oceans. The largest heat transfer from the surface of the oceans (as well as the heat loss due to evaporation) occurs in the western and northwestern regions of the oceans of the northern hemisphere. Here the turbulent heat flux exceeds 40 kcal/(cm² · year). In the more southerly regions, especially close to the equator, where the temperature differences between the surface waters and the air currents above them are small throughout the year, the turbulent heat flux from the surface of the oceans is less than 10 kcal/(cm² · year).

In the southern hemisphere there are no sharp contrasts between the water-air temperatures, and the turbulent flux is much less than in the northern hemisphere, and nowhere exceeds 15 kcal/(cm² · year).

The negative yearly sums of turbulent heat exchange with the atmosphere (i.e., heat inflow from the atmosphere) are observed in the zones of the cold California currents and the currents of the westerly winds in the southern hemisphere. In absolute values these negative quantities of the turbulent heat flux are small.

/32

Just as for the heat loss to evaporation, the yearly sums of the turbulent heat exchange with the atmosphere are derived mainly from values in the autumn-winter period. The closest connection between the conditions of heat exchange with the influence of the sea currents and the atmospheric circulation is observed in the winter. The heat loss by the oceans in the winter months in the northern hemisphere is 8-10 kcal/(cm² · month); and in the southern hemisphere it is about 5 kcal/(cm² · month).

In the summer months for both hemispheres the turbulent heat exchange between the surface of the oceans and the atmosphere is everywhere close to zero. Its absolute values range from 1 to -1 kcal/(cm² · month).

Table 10 gives the average latitudinal values of the turbulent heat exchange between the Earth's surface and the atmosphere, obtained from the map shown in Figure 4 and the data in "Atlas of the Heat Balance of the Earth" [6].

As may be seen from this table, the values of the turbulent heat flux change very little. In the majority of the latitudinal zones of the ocean, the new values are somewhat higher. The decrease in the turbulent heat flux to the south of 40° south latitude for the oceans may be explained by the fact that, based on the results of the present study, at the moderate latitudes of the southern hemisphere, there are regions where the turbulent heat flux is directed from the atmosphere to the surface of the ocean.

/33

TABLE 10. AVERAGE LATITUDINAL VALUES OF THE TURBULENT HEAT EXCHANGE BETWEEN THE EARTH'S SURFACE AND THE ATMOSPHERE. $\text{KCAL}/(\text{CM}^2 \cdot \text{YEAR})$

Latitudinal zone . .	Land		Oceans	
	1963	1973	1963	1973
70--60° N	6	6	16	22
60--50	11	9	16	19
50--40	21	20	14	16
40--30	37	35	13	14
30--20	49	45	9	7
20--10	42	42	6	7
10--0	24	22	4	7
0--10° S	22	18	4	6
10--20	32	30	5	9
20--30	42	43	7	11
30--40	34	33	9	11
40--50	20	22	9	6
50--60	11	13	8	9
Earth as a whole	24	23	8	9

3.5. Heat Exchange Between the Surface of the Ocean and the Underlying Water Layers.

Due to the action of the currents, the values of the heat exchange between the ocean surface and the deeper layers are determined just as when formulating the map of "Atlas of the Heat Balance" [5] by algebraic summation of the values for the radiation balance, heat loss to evaporation and turbulent heat exchange between the ocean surface and the atmosphere. Thus, the algebraic sum of the terms of the heat balance equation for the world's ocean as a whole is 2% with respect to the value of the radiation balance, which indicates the reliability of these methods for calculating the components of the heat balance for the oceans. The indicated discrepancy in the heat balance equation for the world's oceans was removed when formulating the map for heat loss to evaporation and turbulent heat exchange with the atmosphere.

Figure 5 shows a yearly map of the residual term of the heat balance equation - heat obtained or lost by the surface of

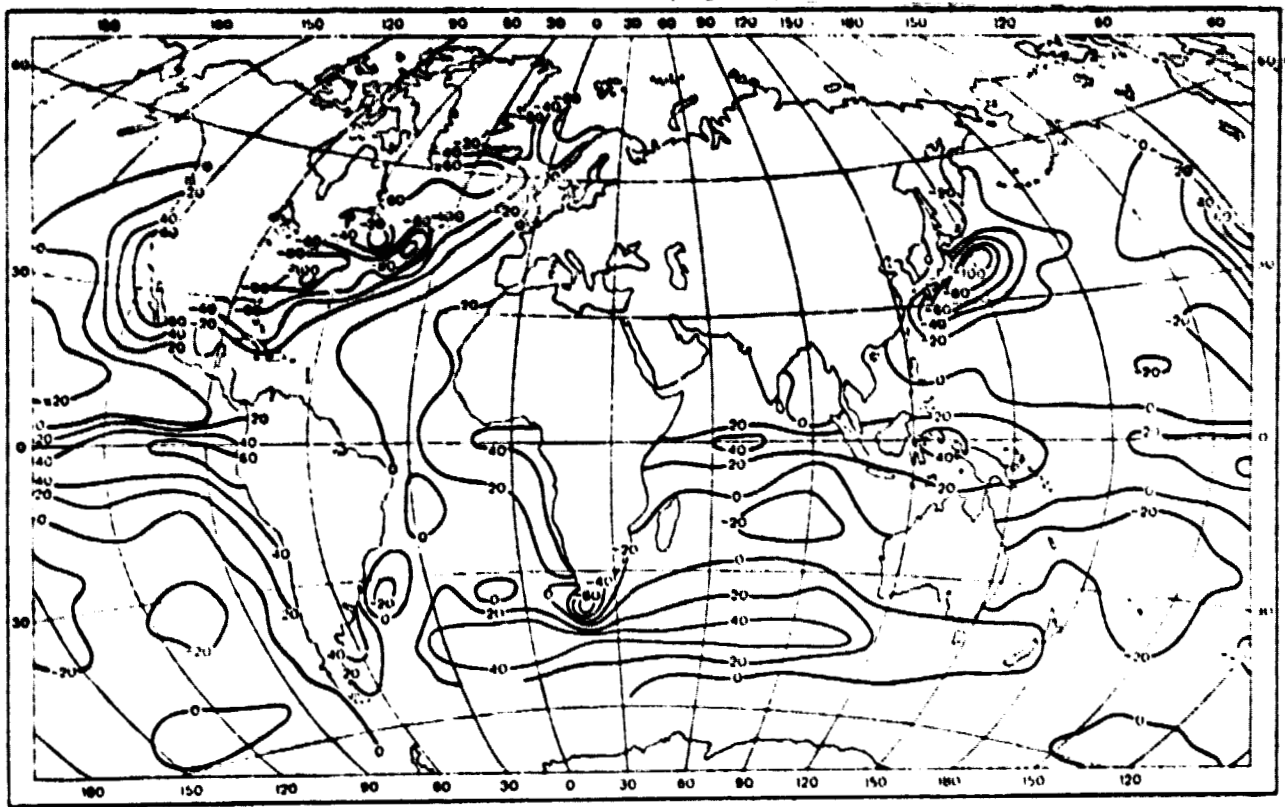


Figure 5. Heat flux is positive from ocean surface to underlying water layers.

ORIGINAL PAGE IS
OF POOR QUALITY

the oceans due to the action of the sea currents. This map shows the role of the currents and atmospheric circulation in the thermal interaction of the surface waters of the oceans with the underlying water layers. At the same time this map characterizes the redistribution of heat between different ocean regions.

It may be seen that in the equatorial and partly at the tropical latitudes of both hemispheres, as a result of large inflow of radiation heat and its low loss to evaporation, the turbulent heat exchange between the atmosphere and the oceans reaches 20-40 kcal/(cm² · year). In the direction of the higher latitudes of both hemispheres, there is a decrease in the accumulation of heat by the oceans. Here the amount of radiation heat is insufficient to cover the heat loss to evaporation and turbulent heat transfer. Therefore heat from the lower layers carried by the currents reaches the surface of the oceans. The regions for the largest release of heat by the waters to the atmosphere lie in the regions affected by the thermal currents - the Gulf Stream and the Curacao. In these regions in the cold part of the year, there is an interaction between the thermal waters of the ocean and the currents of the cold continental air of North America and Asia. This produces conditions for intense transfer of heat by the deeper layers of the ocean waters through the surface of the ocean into the atmosphere, reaching 110 kcal/(cm² · year).

It must be noted that at the high and moderate latitudes of the northern hemisphere, due to large temperature contrasts in the water and the air, a similar process takes place in the regions affected not only by the thermal currents but also certain cold currents.

In the southern hemisphere where the temperature contrasts between the water-air are much less the heat loss from the surface of the ocean does not exceed - 30, -35 kcal/(cm² · year). /35

In the regions influenced by the cold currents of both hemispheres (except for the regions indicated above), the surface waters receiving heat from the Sun and the atmosphere transfer a large portion of it to the deeper layers. The largest amount of heat is received in the depths of the ocean in the region of the California currents - about $60 \text{ kcal}/(\text{cm}^2 \cdot \text{year})$. In the southern hemisphere the surface waters of the Peru, Bengel and Falkland currents and the currents of the westerly winds transfer a much smaller amount of heat to the lower lying layers - up to $50 \text{ kcal}/(\text{cm}^2 \cdot \text{year})$.

In compiling the average latitudinal values of heat exchange between the ocean surface and the underlying layers, based on the results of new and previous calculations (Table 11), one can observe great differences in the latitudinal behavior of this component of the heat balance for the oceans in both hemispheres.

TABLE 11. AVERAGE LATITUDINAL VALUES OF HEAT EXCHANGE BETWEEN THE OCEAN SURFACE AND UNDERLYING LAYERS $\text{KCAL}/(\text{CM}^2 \cdot \text{YEAR})$.

Latitudinal zone			Latitudinal zone		
	1963	1973		1963	1973
70-60° N	-26	-33	0-10° S	27	22
60-50	-26	-24	10-20	4	0
50-40	-16	-20	20-30	-6	-8
40-30	-16	-20	30-40	-7	-1
30-20	-1	-5	40-50	-7	15
20-10	14	-3	50-60	-11	3
10-0	31	13	Ocean as a whole	0	0

In contrast to the results obtained previously, in the northern hemisphere there is a smaller accumulation of heat at the tropical latitudes due to an increase in its loss to evaporation. In the southern hemisphere heat enters the depths of the ocean at the extratropical latitudes, which requires further research, since meteorological and hydrological regimes at these latitudes have not been studied adequately.

4. Heat Balance of the Earth

Data on the distribution of the heat balance components make it possible to determine the values of these components for the Earth.

Table 12 gives the values of the heat balance components of the Earth for different latitudinal zones of land and oceans./36 The last column of this table contains information on the heat balance of the Earth as a whole.

TABLE 12. AVERAGE LATITUDINAL VALUES OF THE HEAT BALANCE COMPONENTS OF THE SURFACE OF THE EARTH(KCAL/(CM² · YEAR))

Latitudinal zone	Land			Oceans				Earth			
	R	LE	P	R	LE	P	F _s	R	LE	P	F _s
70-60° N	22	16	6	23	31	22	-30	22	20	11	-9
60-50	32	23	9	43	47	19	-23	37	33	13	-9
50-40	45	25	20	61	67	16	-19	54	45	18	-9
40-30	58	23	35	90	96	14	-20	76	65	23	-12
30-20	61	19	45	111	109	7	-5	94	75	21	-2
20-10	74	32	42	121	117	7	-3	109	95	16	-2
10-0	79	57	22	124	104	7	13	114	93	10	11
0-10° S	79	61	18	127	99	6	22	116	90	9	17
10-20	75	45	30	122	113	9	0	112	98	14	0
20-30	71	28	43	109	106	11	-8	100	88	18	-6
30-40	62	29	33	92	82	11	-1	89	76	14	-2
40-50	44	22	22	72	51	6	15	71	50	7	14
50-60	35	22	13	46	35	9	2	46	35	9	2
Earth as a whole	50	27	23	91	82	9	0	79	66	13	0

The materials given here may be compared with the results of previous studies on the heat balance of the Earth's surface. Table 13 gives relative values of the heat balance components (expressed in percents of the values for the solar constant), obtained from materials from research in different years.

TABLE 13. HEAT BALANCE OF THE SURFACE OF THE EARTH
(THE BALANCE COMPONENTS ARE GIVEN IN PERCENTS
OF THE AMOUNT OF SOLAR RADIATION REACHING THE
EXTERNAL ATMOSPHERIC BOUNDARY).

Study	Components of balance				
	Absorbed radiation	Effective radiation	Radiation balance	Heat loss due to evaporation	Turbulent heat flux
Dines, 1917	42	14	28	21	7
Alt, 1929	43	27	16	16	0
Baur, Philippines, 1934	43	24	19	23	-4
Houghton, 1954	47	14	33	23	10
Lettau, 1954	51	27	24	20	4
Heat Balance Atlas (1955)	42	16	26	21	5
Heat Balance Atlas for the Earth, (1963)	43	15	28	23	5
Present study	46	15	31	26	5

137

It may be seen from the data given in the last three columns of this table that the refinement of the world maps for the heat balance components has been accompanied by a certain increase in the values of the absorbed radiation, radiation balance and heat loss to evaporation. The relative values of the heat balance components, found in this study, approximate the results obtained in the last 50 years by Houghton (with the exception of the turbulent heat flux).

Using the materials from the last calculation of the heat balance terms, we may refine the heat balance of the Earth as a whole. Assuming the solar constant equals $1.95 \text{ kcal}/(\text{cm}^2 \cdot \text{min})$ and the albedo of the Earth is close to 0.30 we find

Worldwide space

Atmosphere

The Earth's surface

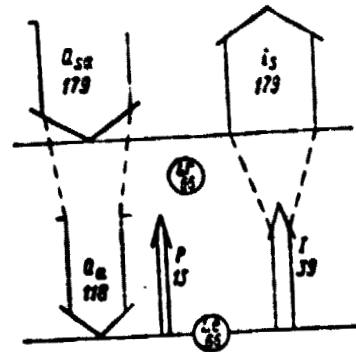


Figure 6. Heat balance of the Earth (component balance in $\text{kcal}/\text{cm}^2 \cdot \text{year}$)).

we find that the value of the solar radiation absorbed by the Earth as a planet equals $179 \text{ kcal}/(\text{cm}^2 \cdot \text{year})$ (the arrow Q_a in figure 6). Out of this amount, $118 \text{ kcal}/(\text{cm}^2 \cdot \text{year})$ is absorbed on the surface of the Earth (arrow Q_s), and $61 \text{ kcal}/(\text{cm}^2 \cdot \text{year})$ is absorbed in the atmosphere.

The radiation balance of the Earth's surface equals $79 \text{ kcal}/(\text{cm}^2 \cdot \text{year})$, and the effective radiation from the surface of the Earth, corresponding to the difference between the absorbed radiation and the radiation balance, is $39 \text{ kcal}/(\text{cm}^2 \cdot \text{year})$ (arrow I).

The total value for the long wave radiation of the Earth, which reaches the regions above the seas, equals the amount of absorbed radiation designated by the arrow I_s . The ratio I/I_s is much less than the ratio Q_a/Q_{sa} , which characterizes the influence of the greenhouse effect upon the radiation regime of the Earth. Another characteristic of the greenhouse effect is the value of the radiation balance of the Earth's surface which equals $79 \text{ kcal}/(\text{cm}^2 \cdot \text{year})$.

/38

The energy of the radiation balance is consumed in the evaporation of water ($66 \text{ kcal}/(\text{cm}^2 \cdot \text{year})$, expressed in the form of a circle LE) and on turbulent heat exchange of the Earth's surface with the atmosphere ($13 \text{ kcal}/(\text{cm}^2 \cdot \text{year})$, arrow P). The atmosphere receives thermal energy from three sources: absorbed short wave radiation ($61 \text{ kcal}/(\text{cm}^2 \cdot \text{year})$), heat inflow from the condensation of water vapor ($66 \text{ kcal}/(\text{cm}^2 \cdot \text{year})$, expressed by the circle LR), and turbulent heat flux from the Earth's surface ($13 \text{ kcal}/(\text{cm}^2 \cdot \text{year})$). The sum of these values equals the heat loss to long wave radiation in space, which equals the difference I_s and I, i.e. $140 \text{ kcal}/(\text{cm}^2 \cdot \text{year})$.

References

1. Aktinometricheskiy spravochnik. Zarubezhnyye strany (Actinometric handbook. Foreign countries). Edited by T. G. Berlyand, Leningrad, Gidrometeoizdat, 1964.
2. Ariel', N.Z. - et al. Calculations of average monthly values of fluxes of heat and moisture over the ocean. Meteorologiya i Gidrologiya, 1973, No. 5, pp.3-11.
3. Atlas Antarktii (Atlas of Antarctica). Moscow, Leningrad, 1966.
4. Atlas okeanov. Tikhyy okean (Atlas of the Oceans. Pacific Ocean) 1974.
5. Atlas teplovogo balansa. (Atlas of Heat Balance) Edited by M.I. Budyko Leningrad, 1955.
6. Atlas teplovogo balansa zemnogo shara (Atlas of the Heat Balance of the Earth). Edited by M. I. Budyko, Moscow, Mezhvedomstvennyy geofizicheskiy komitet, 1963.
7. Beyeva, I. M., Kirillova, T. V., Strokina, L. A. Method of allowing for influence of cloudiness on total radiation in climatic calculations. Tr. GGO, 1975, No. 338, pp. 68-72.
8. Berlyand, M., Berlyand, T. Determination of effective radiation considering influence of cloudiness. Izvestiya AN SSSR. Seriya geofiz. 1952, No. 1, pp. 64-78.
9. Berlyand, T.G. Method of climatological calculations of total radiation. Meteorologiya i gidrologiya, 1960, No. 6, pp. 9-12.
10. Berlyand, T. G. Distribution of solar radiation on the continents. Leningrad, Gidrometeoizdat, 1961, 227 pages.
11. Berlyand, T. G. Solar radiation regime on African Territory Tr. GGO, 1971 No. 287, pp. 3-34.
12. Berlyand, T. G. Radiation regime of Non-USSR Asia. TR. GGO, 1971, No. 287, pp. 3-34.
13. Bortkovskiy, R. S. Calculation of turbulent fluxes of heat, moisture, and momentum above the sea from ship measurements. Meteorologiya i gidrologiya, 1971, No. 3, pp. 93-98.
14. Bortkovskiy, R. S. Influence of hurricanes on macro-scale interaction of the ocean and atmosphere. Tr. GGO, 1972, No. 297, pp. 78-82.
15. Budyko, M.I. Tepovoy balans zemnoy poverkhnosti (heat balance of the earth's surface). Leningrad, Gidrometeoizdat, 1956, 255 pp.

16. Budyko, M. I. *Klimat i zhizn'* (Climate and life). Gidrometeoizdat, 1971, 472 pages.
17. Budyko, M. I. Zubenok, L. I. Determination of evaporation from the land surface. *Izvestiya AN SSSR. Seriya geogr.*, 1961, No. 6., AN pp 3-17.
18. Verigo, S. A., Razumova, L. A. *Pochvennaya vlaga i yeye znacheniye v sel'skokhozyaystvennom proizvodstve* (Soil moisture and its importance in agriculture). Leningrad, Gidrometeoizdat, 1963, 289 pp.
19. Girdyuk, G. V., et al. Transparency of the atmosphere above the ocean and sum of possible radiation. *Tr. GGO*, 1973, No. 297. pp. 99-108.
20. Girdyuk, G. V., Kirillova, T. V. Method for calculating the components of the radiation balance of the ocean surface. *Meteorologiya i gidrologiya*, 1974, No. 12, pp. 63-69.
21. Yefimova, N. A. Method for calculating the monthly values of effective radiation. *Meteorologiya i gidrologiya*, 1961, No. 10, pp. 28-33.
22. Yefimova, N. A., Strokina, L.A. Distribution of the effective radiation on the surface of the earth. *Tr. GGO*, 1963, No. 139, pp. 16-26.
23. Yefimova, N. A. *Radiatsionnyye faktory produktivnosti rastitel'nogo pokrova* (Radiation factors of the productiveness of vegetation). 1977, 225 pages.
24. Zubenok, L. I. *Ispareniya na kontinentakh* (Evaporation on the continents). Leningrad, Gidrometeoizdat, 1976, 264 pp.
25. *Karty srednego godovogo stoka rek SSSR. Prilozheniye k monografii K. P. Voskresenskogo "Norma i izmenchivost' godovogo stoka rek Sovetskogo Soyuz"* (Map of the yearly average discharge of USSR rivers. Appendix to the monograph of K. P. Voskresenskiy: Norm and changes of the yearly discharge of the Soviet Union rivers). Leningrad, Gidrometeoizdat, 1967, 546 pp.
26. Kirillova, T. V. Albedo of the oceans. *Tr. GGO*, 1972, No. 282 pp. 215-219.
27. *Klimaticheskiy spravochnik Avstralii i Novoy Zelandii* (Climatic Handbook of Australia and New Zealand). Edited by A. Yu. Yegorov and P. S. Borushko. Leningrad, Gidrometeoizdat, 1975, 144 pages.
28. *Klimaticheskiy spravochnik Yuzhnoy Ameriki* (Climatic Handbook of South America). Edited by A. N. Lebedev. Leningrad, Gidrometeoizdat, 1975, 370 pages.

29. Kuz'min, P. P. Theoretical scheme for determining errors in calculating evaporation from land surface. In the book: Materials of the interdepartmental conference on studying and validating methods of calculating evaporation from a water surface and land, 3-7 August 1965, Valdau, 1966, pp. 271-283.
30. Marshunova, M.S., Chernigovskiy, N.T. Radiatsionnyy rezhim Zarubezhnoy Arktiki (Radiation Regime of the Non-USSR Arctic). Leningrad, Gidrometeoizdat, 1971, 182 pages.
31. Mirovoy vodnyye balans i vodnyye resursy zemli (World Water Balance and Water Reserves of the Earth). Leningrad, Gidrometeoizdat, 1974, 638 pages.
32. Ogneva, T. A. Relationship of thermal balance components in the Soviet Union. Tr. GGO, 1968, No.233, pp. 110-117.
33. Rekomendatsii po raschetu sostavlyayushchikh radiatsionnogo balansa poverkhnosti okeana (Recommendations on calculating components of the radiation balance of the ocean surface. Leningrad, Izd. GGO, Murmansk Branch of the AANII, 1974, 14 pages.
34. Rukovodstvo po gradientnym nablyudeniyam i opredeleniyu sostavlyayushchikh teplovogo balansa (Handbook on gradient observations and determination of thermal balance components). Leningrad, Gidrometeoizdat, 1964, 129 pages.
35. Sivkov, S. I. Metody rascheta kharakteristik solnechnoy radiatsii (Methods of calculating solar radiation characteristics) Leningrad, Gidrometeoizdat, 1968, 32 pages.
36. Solnechnaya radiatsiya i radiatsionnyy balans (Mirovaya set') (Solar radiation and the radiation balance, world-wide network). 1964-1974, Leningrad, Izd. GGO, 1965-1975.
37. Spravochnik po klimatu SSSR (Handbook on USSR Climate). Chapter I, Leningrad, Gidrometeoizdat, 1968.
38. Ibid, Chapter II, Leningrad, Gidrometeoizdat, 1964-1967.
39. Ibid, Chapter IV, Leningrad, Gidrometeoizdat, 1967-1970.
40. Sredniye mnogoletniye mesyachnyye i godovyye summy atmosferykh osadkov po zarubezhnoy territorii severnogo polushariya (Average multi-year monthly and yearly sums of atmospheric precipitation on foreign regions of the northern hemisphere). Edited by O. A. Drozdov. Leningrad, Gidrometeoizdat, 1972, 92 pages.
41. Srednyaya mnogoletnyaya temperatura vozdukh po zarubezhnoy territorii i akvatorii severnogo polushariya (Average multi-year air temperature on foreign territories and water areas of the northern hemisphere). Edited by V. Ya. Sharova. Leningrad, Gidrometeoizdat, 1970, 148 pages.

42. Strokina, L. A., Khrol, V. P. Fresh water balance of the world oceans (evaporation). In the book: Mirovoy vodnyy balans i vodnyye resursy zemli (worldwide water balance and water reserves of the earth). Leningrad, Gidrometeoizdat, 1974, pp. 544-550.
43. Alt, E. Status of the meteorological radiation problem. Meteorol. Ztsch, 1929, Vol. 46, No. 12.
44. Angstrom, A. Note on the relation between time of sunshine and cloudiness in Stockholm 1908-1920. "Arch. f. Matemat. Astronom. och. Phys.", 1922, Vol. 17, N 15.
45. Baur, F., Philips, H. Heat management of the air mantle of the northern hemisphere. Gerlands Beitr. z Geoph. 1934, Vol 42.
46. Dines W. H. The heat balance of the atmosphere. "Quart. J. Roy. Met. Soc.", 1917, vol. 43, N 151.
47. Houghton H. G. On the annual heat balance of the Northern Hemisphere. "J. Met." 1954, vol. 11 N 1.
48. Lettau H. A. Study of the mass, momentum and energy budget of the atmosphere - "Arch. f. Met., Geoph u. Biokl., Ser. A" 1954, Bd. 7.
49. Oguntoyinbo, J. S. Reflection coefficient of natural vegetation, crops and urban surfaces in Nigeria. "Quart. J. Roy. Met. Soc.", 1970, vol. 96, N 409, p. 430-441.
50. Tables of temperature, relative humidity and precipitation for the world. p. 1 - IV. London, 1958.
51. U. S. Navy Marine Climatic Atlas of the World, vol. I-V, 1955-1959.